FEM Modeling of Squeeze Film Damping Effect in RF-MEMS Switches

Syed Turab Haider
Department of Electrical Engineering
National University of Sciences and Technology
Islamabad, Pakistan
turabhaider79@ee.ceme.edu.pk

Muhammad Mubasher Saleem
Department of Mechatronics Engineering
National University of Sciences and Technology
Islamabad, Pakistan
mubasher.saleem@ceme.nust.edu.pk

Mashhood Ahmad
Department of Electrical Engineering
National University of Sciences and Technology
Islamabad, Pakistan
mashhood_ahmad@ceme.nust.edu.pk

***Abstract*—A very important aspect in the design of RF-MEMS switches, is to obtain low switching time. The switching time not only depends on the device geometric parameters but also on the operating conditions. This paper presents the squeeze film damping effect on the dynamic response of the RF-MEMS switches. The squeeze film damping effect, with and without perforations, on the switching time is analyzed using finite element method (FEM) simulations. The effect of temperature and humidity on the squeeze film damping and switching time is also investigated.**

Keywords— RF-MEMS, squeeze film air damping, dynamic response, finite element method

I. INTRODUCTION

The presence of thin air film in the suspended vibrating structures, such as plates and beams, strongly affects the dynamic response of the MEMS devices. The air gap between the parallel plates, for the electrostatically actuated RF-MEMS switches, is generally in the range of a few micrometers. This small air gap results in the surrounding air to be squeezed in or out with a displacement of the top suspended plate. This leads to a specific distribution of the air pressure underneath the moving plate depending on the plate geometry and the viscosity of the air. This air pressure distribution generates a force which opposes the plate motion and is generally termed as squeeze film air damping.

The switching time of an RF MEMS switch is strongly influenced by the air damping. For the exact modeling of switching time, at the design level, both the structural parameters and air dissipation mechanism must be considered. The main challenge in the modeling of air damping in MEMS is the presence of irregular geometries and nonlinear fluid interactions. The fluidic non-linearities associated with thin air films in RF-MEMS switches are the viscous or elastic behavior of the air depending on the device operating frequency. Usually, at lower frequencies viscous dissipative or damping effects prevail because of the friction of gas molecules with vibrating surfaces. At higher operating frequencies, elastic effects are dominant where the gas inertial effects prevent the motion of molecules through the structure [1]. Thus the structural parameters such as oscillation at resonant frequency, quality factor, and dynamic response are all influenced by the air damping [2]. The air damping is also strongly influenced by the pressure and rarefaction, as well as by the air fluid properties like temperature, humidity, and viscosity.

The pressure distribution under the suspended plate of an RF-MEMS switch and its effect on the quality factor is analyzed in [3]. The air damping dependence on the resonant frequency of a clamped-clamped microbeam is presented in [4]. The effect of squeeze film damping with an alternating actuation voltage for an electrostatically actuated RF-MEMS switch is discussed in [5]. Reference [6] studied the behavior of micro curved beam with the effects of squeeze film damping, assuming the general Reynolds equation form. Liu *et al.* [7] studied the dynamic behavior of damping effect on an electrostatically actuated circular plate. Reference [8] provided an experimental validation of air damping in the free molecule regime using a parallel-plate microstructure operated at variable pressure conditions. The analyses by Hosseinian *et al.* [9] show that air viscosity and air density affect the quality factor of a MEMS resonator operating in an atmospheric air environment. The quality factor was evaluated based on air damping for multiple humid environments.

In this paper, the thin film air pressure distribution in the electrostatic symmetric toggle RF-MEMS switch (STS) with and without air perforations, in the suspended plate, is presented. Moreover, the air damping effect on the switching time of the STS switch under varying device operating conditions is analyzed. This paper describes the STS switch designs and the operating principle in section II. Section III describes the pull-in mechanism and switching time being a function of the applied actuation voltage and pull-in voltage. In section IV, FEM analysis consisting of pressure distribution, switching time, and effects of temperature and humidity on the switching time are simulated.

II. THE STS SWITCH DESIGN AND OPERATING PRINCIPLE

Farinelli *et al.* [10] presented an STS MEMS switch for low pull-in voltage and high mechanical stability. The bias electrodes mounted on the outer and inner sides of the switch are termed as pull-out and pull-in electrodes respectively.

978-1-5386-0549-3/17/$31.00 ©2017 IEEE

When the bias voltage at the pull-in electrodes is higher than a threshold value, the central bridge comes in contact with the transmission line due to the pull-in phenomenon. This moves the STS switch to the off-state. Fig. 1 shows the schematic diagram of the STS RF-MEMS switch. The switch design is mounted on a 50 Ω coplanar waveguide (CPW) and consists of a gold electroplated suspended structure fixed to the substrate by the four torsion springs. The thickness of the movable top plate and central bridge area is further increased by a second gold layer to increase the overall stiffness. The polysilicon electrodes at the bottom are fabricated with a thickness of 0.63 µm. The suspended top electrode is perforated with circular holes. The presence of the perforations helps an easy etching of the sacrificial layer with a final air gap thickness of 3 µm between the bottom fixed polysilicon and the top suspended electrode electrode. In this paper two switch designs, with and without etch holes, are considered for the analysis of squeeze film air damping. Table. I shows the design parameters of the two STS switch designs.

TABLE. I. DESIGN PARAMETERS OF THE TWO STS SWITCHES.

Parameters	Switch design 1	Switch design 2
Top electrode length (µm)	210	210
Top electrode width (µm)	90	90
Top electrode thickness (µm)	4.8	4.8
Connecting lever length (µm)	30	30
Connecting lever width (µm)	10	10
Connecting lever thickness (µm)	1.8	1.8
Air gap thickness (µm)	3	3
Holes radius/pitch (µm)	5/10	----
Torsion spring length (µm)	30	30
Torsion spring width (µm)	10	10
Torsion spring thickness (µm)	1.8	1.8

III. SWITCHING TIME AND PULL-IN VOLTAGE OF STS SWITCH

The STS switch design, shown in Fig. 1, uses torsion actuators which have one degree of rotational freedom around the torsion spring axis. At a certain actuation voltage, the electrostatic torque increases than the mechanical torque and the top suspended plate snaps down. This actuation voltage is termed as “pull-in voltage". The pull-in voltage for the STS switch, in terms of structural parameters, can be derived as [10];

$$V_p = \sqrt{\frac{E}{2.3\,\varepsilon_0 W}\left(\frac{h_o}{L}\right)^3 \left(\frac{0.33}{1-v}\frac{b_t {h_t}^3}{l_t} + \frac{L}{l_c^2}\frac{b_c {h_c}^3}{6}\right)} \quad (1)$$

Where b_t, h_t, l_t, b_c, h_c, l_c are the width, thickness, and length of torsion springs and connecting levers, respectively, W and L are the top electrode width and length respectively, E is the Young’s modulus, h_o is the initial air gap between the suspended plate and fixed polysilicon electrode, v is the Poisson ratio and ε_0 is the permittivity of free space.

The switching speed of an electrostatically actuated parallel plate RF-MEMS switch depends on the actuation voltage. Generally, the actuation voltage is 1.3-1.4 times the pull-in voltage to obtain fast switching time [11]. A very large switching voltage will result in a strong electrostatic force, thus leading to high switching speed. The expression for the switching time of the parallel plate RF-MEMS switches is given by [11]

$$t_{pi} = \frac{3.67 V_p}{\omega\, V_s} \quad (2)$$

Where ω is the resonant frequency, V_s is the actuation voltage, and V_p is the pull in voltage. For the air-damped case, the switching time is dependent on the switch quality factor Q and is given as;

$$t_{pi} = \frac{9\, V_p^2}{4\,\omega\, Q\, V_s^2} \quad (3)$$

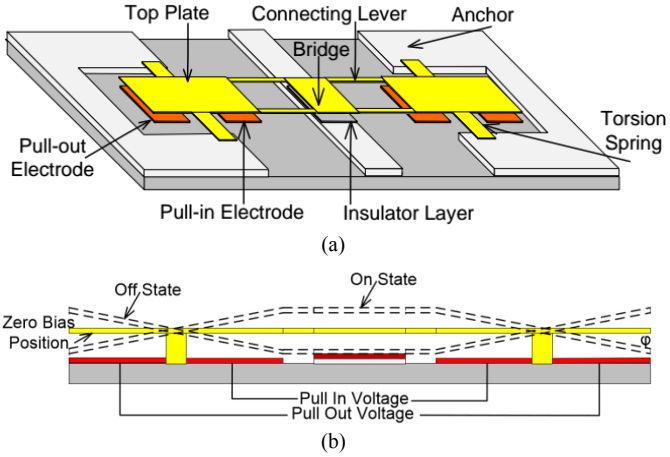

Fig. 1. (a) Showing the 3D schematic and (b) side view of the STS switch

IV. FEM BASED SQUEEZE FILM DAMPING ANALYSIS

The thin air film modeled for the STS switch considered in this paper lie parallel to the bottom plate. As the switch moves towards the substrate during an electrostatic pull-down, the gap between the suspended plate and fixed polysilicon electrode decreases causing air to be squeezed. Upon release of the actuation voltage, the plate moves towards its restoring direction. The air gap consequently enlarges, which creates an air flow motion directed towards the central portion of the plate. In both cases of voltage biasing, the air flow underneath the suspended plate exerts forces due to the air pressure distribution. The plate movement is always opposed by the underneath air gap. To model the pressure distribution under the rotating top plate a modified Reynolds equation of the air distribution in the direction normal to the bottom plate can be modeled as [12];

$$\frac{d^2p}{dx^2} + \frac{d^2p}{dy^2} = \frac{12\mu_{eff}}{h_0^3}\frac{d(ph_0)}{dt} \quad (4)$$

Where h_0 is the gap thickness, $p(\mathrm{x},\mathrm{y})$ is the pressure inside the air gap and $p(\mathrm{x},\mathrm{y}) = P_a + \mathrm{p}'(\mathrm{x},\mathrm{y})$, where P_a is the

ambient pressure and $p'(x,y)$ is pressure due to the squeeze film effect, μ_{eff} is the air effective viscosity which takes account of the rarefaction effects. The analytical models presented by the Bao *et al.* [12] and Pandey *et al.* [13] explain the squeeze film damping due to the out-of-plane motion between the two parallel plates.

A. Pressure Distribution Analysis

To model the air film underneath the STS switches and to observe the resulting damping parameters, the ANSYS FEM model is used. The FEM model consists of two different steps: the first step produces the air model present below the movable switch, whereas the second step models the air film in each perforation. The thin air film separating the movable switch plate from the fixed plate is modeled with the *fluid* 136 elements. In each air hole, the air flow is modeled by the *fluid* 138 elements, which is a one-dimensional element and has two nodes. The *fluid* 138 elements estimate the pressure gradients at the hole's borders. The lower node of *fluid* 138 elements is coupled with the *fluid* 136 element nodes at the edges. The fluidic domains are defined by a set of variables the corresponding reference pressure, the ambient pressure, the mean free path, and the air gap thickness.

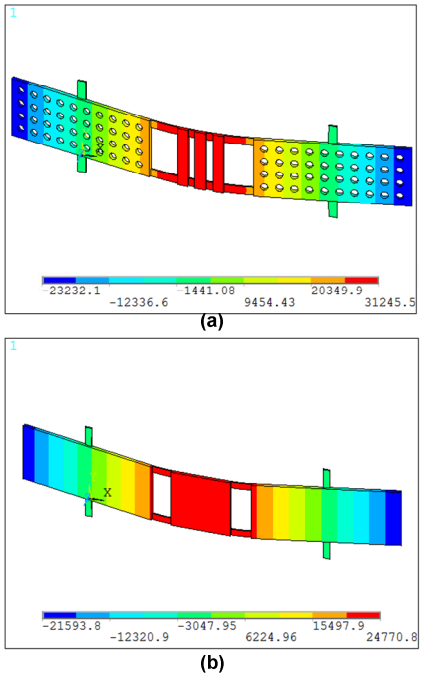

Fig. 2. First resonant frequency mode shape (a) switch design 1 with air holes (b) switch design 2 without air holes.

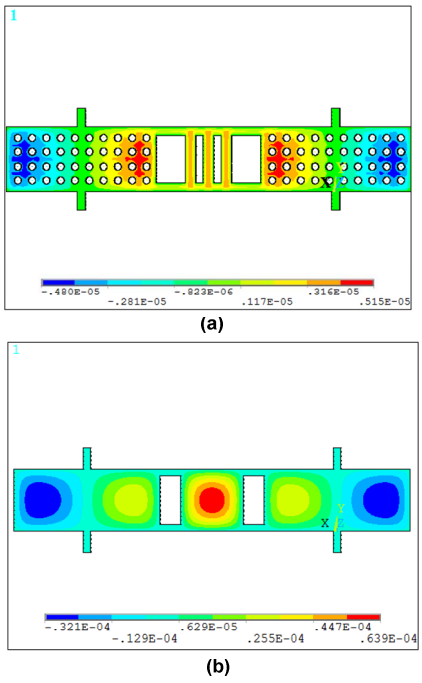

Fig. 3. Pressure distribution for the (a) switch design 1 with air holes (b) switch design 2 without air holes.

The technique we used for evaluating damping parameters is modal projection analysis. The modal projection technique is implemented after the formation of fluid elements and using a solid structure to provide information on the Eigen-frequencies and mode shapes. For each Eigen-frequency called an Eigen-mode, we imposed the distributed vectors as velocity loads and computed the resulting pressure distribution and hence the damping parameters acting on the structure. The simulated 1st resonant modes for the switch design 1 and switch design 2 are 14.4 kHz and 12.8 kHz respectively, as shown in Fig. 2. The corresponding damping coefficient at the 1st resonant frequency is 2.459 µN.s/m and 11.813 µN.s/m for switch design 1 and switch design 2 respectively. The resulting damping ratio is 0.00387 and 0.0174 for the switch design 1 and switch design 2 respectively.

Fig. (3a) and Fig. (3b) show the pressure distribution under the 1st resonant mode for the switch design 1 and switch design 2 respectively. The pressure distribution contours can be described by the movement of the central bridge and the top suspended plate. Under the 1st resonant mode the central bridge moves upward, causing air to be squeezed in, thus air concentration is observed at the central bridge. For the switch design 1, as seen in Fig. (3a), the observed pressure distribution has a lower magnitude because the central bridge is perforated and has wider air channels to allow air to escape though, thus the magnitude will decrease. The pressure distribution also indicates that the air distribution acting on the connecting lever is considerable in the case of perforations. The pressure distribution under the case of switch design 2 as shown in Fig. (3b) forms wider contours and the pressure acting on the

connecting lever is negligible, thus the whole air concentration is around the central bridge and the top electrode plate.

B. Rarefied Gas Effects

For the STS switch design, the gas rarefaction effects are considered in the air gap between the oscillating plate and the bottom fixed electrode and in the air flow through the holes. The rarefied gas effect is modeled using the Knudsen number (K_n). For the air gap between the plates K_n is defined as λ/h_0, where λ is the gas molecules mean free path and h_0 is the air gap. The Knudsen number for the air flow through the perforation is λ/r, where r is the air hole radius. Based on the gap thickness, the value of K_n gives information about the possible air flow regime which is shown in Table. II. In our case, the gap between the suspended plate and the bottom fixed electrode for the STS switch is 3 µm with a K_n value of 0.021 for the air gap and 0.0126 for the air hole. The values show that the regime of operation for the STS switch is the slip flow regime.

TABLE.II KNUDSEN NUMBER CLASSIFICATION

Continuum flow	$K_n < 10^{-2}$
Slip flow	$10^{-2} < K_n < 10^{-1}$
Transition flow	$10^{-1} < K_n < 10$
Free molecular flow	$K_n > 10$

The rarefied gas effects are included in the effective viscosity coefficient μ_{eff} which is;

$$\mu_{eff} = \frac{\mu_a}{Q_{pr}} \tag{5}$$

Where Q_{pr} is the relative flow rate coefficient and $\mu_a$is the absolute air viscosity. The flow rate coefficient is a function to K_n. For the slip flow regime, $Q_{pr} = 1 + 9.638\, K_n^{1.1}$ [14].

C. Compressibility

For the designed switches the measure of the compressibility is termed by the squeeze number σ, which is given as

$$\sigma_l = \frac{12\mu_a \omega L^2}{P_a\, h_0^2} \tag{6}$$

where, P_a is the ambient pressure. For the air holes in the switch, the squeeze number is defined as

$$\sigma_r = \frac{12\mu_a \omega r^2}{P_a\, h_0^2} \tag{7}$$

where, r is the radius of the air hole and is almost equal to half the holes pitch. The compressibility is dependent on the square of the lateral dimension to the air gap thickness (L/h_0) ratio, oscillation frequency (ω) and inversely proportional to the ambient pressure (P_a). The effect of compressibility should be considered when $\sigma > 1$. The calculated values of squeeze number for both the holes and plate are 0.0025 and 6.138 respectively. Based on the calculated values additional properties of air compressibility should be considered for *fluid* 136 elements to accurately model the air damping effect.

D. Switching time

Fig. (4a) shows the switching time of the switch design 1 with and without considering squeeze film air damping effects. The switching time is also obtained at different ratios of V_s/V_{pi}. The observed pull-in voltages for the switch design 1 and the switch design 2 are 55.12 V and 52.6 V respectively. It can be observed that in the presence of air damping effects the switching time is higher by a value of 2.35 µs and 4.21 µs as compared to switching time without damping effects for the switch design 1 and the switch design 2 respectively. Moreover, for the switch design 1 with the high values of V_s/V_{pi} the switching time decreases by 17.3 µs from $V_s/V_{pi} = 1$ to $V_s/V_{pi} = 2$ without damping effects and 19.23 µs with damping effects. Similarly, Fig. (4b) shows the switching time of the switch design 2 with and without considering squeeze film damping effects. The observed results show a drop of switching time by 24.34 µs for $V_s/V_{pi} = 1$ to $V_s/V_{pi} = 2$ without damping effects and 27.48 µs with damping effects. Also with the higher V_s/V_{pi} ratios the switching times started to converge as the effects of air damping are reduced with increasing voltages. This can also be seen from Eq. (2) and Eq. (3), that switching time follows a linear drop directly related to V_s/V_{pi} but for the air damping, the switching time follows a nonlinear drop directly related to V^2_s/V^2_{pi}.

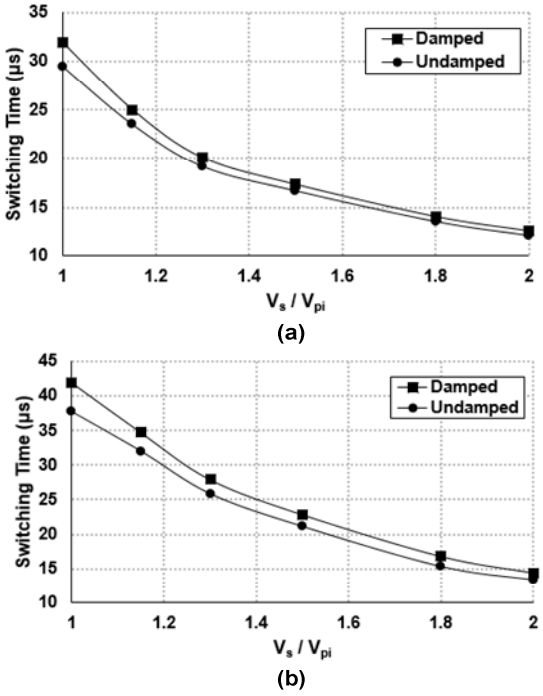

Fig. 4. Switching time simulation of the designed STS switches for different V_s/V_{pi} for (a) switch design 1, (b) switch design 2

E. Effects of Humidity and Temperature

For the two STS switch designs, we considered the combined effects of humidity and temperature to model the change in the dynamic viscosity of the fluid elements. The dynamic values of air viscosity were taken as a parameter to model the switching time. The thermophysical properties of air at 25°C to 100°C temperatures, for dry and humid environments, are evaluated in [15]. Fig. 5 shows μ_{eff}, as a function of relative humidity or RH and temperature. The effect of relative humidity and temperature on switching time is shown in Fig. 6(a) and Fig. 6(b) for the STS switch design 1 and switch design 2. The designs are simulated from 25°C to 100°C for 0% to 100% humidity with an increment by 50 %. The simulated switching time value depends both on the humidity and temperature. For a certain temperature, switching time increases with decreasing humidity, the reason being an increase in the air viscosity thus increasing damping. For both the STS switches, switching time is largest at 100° C for dry air or RH = 0 % and smallest at 100° C for RH = 1.

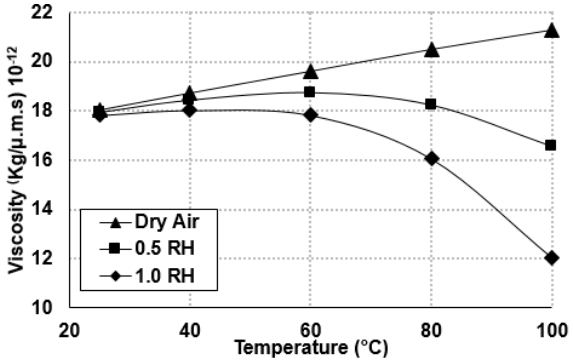

Fig. 5. Effective viscosity of moist air as a function of relative humidity and temperature

The FEM results show that the higher value of humidity level decreases the switching time by 1.83% for RH = 0.5 and 3.81% for RH = 1 for the switch design 1. Similarly, a higher value of humidity level consequently decreases the switching time by 3.58 % for RH = 0.5 and 6.45 % for RH = 1 for the switch design 2. The variation in the switching time is nonlinear under temperature variation of 25° C to 100° C for different humidity levels but linear under the case of dry air.

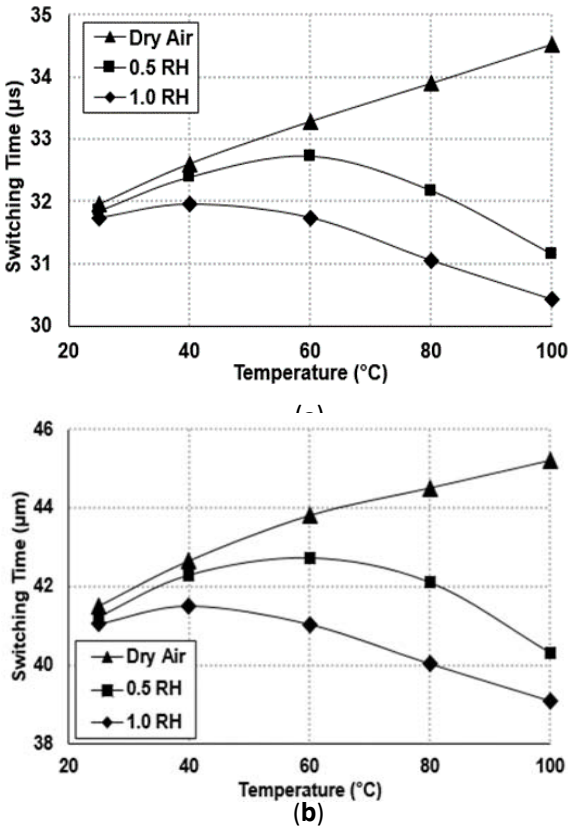

Fig. 6. Switching time as a function of temperature and RH for (a) switch design 1, (b) switch design 2

V. CONCLUSION

In this paper, we demonstrated an FEM study of squeeze film air damping effects on the switching time for a symmetric toggle RF-MEMS switch. The FEM models in this study presented are derived using the modal projection method in ANSYS. In conclusion, this study shows the need to consider the effect of switching operating conditions on the switching time of the designed switches. The air damping model, simulates the switching time from 25°C, RH = 0 to 100°C, RH = 1. In high humid environments, the switching time can decrease by 1.5 μs for the switch design 2 and 0.5 μs for the switch design 1 respectively. The switching time is also dependent on the pull-in voltage to the applied voltage ratio and as the generated electrostatic force for pull-in increases with the applied voltage, the switch takes a shorter duration for the movement. A difference of 17.3 μs and 24.34 μs is observed for the switch design 1 and switch design 2 respectively, for the ratio of $V_s/V_{pi} = 1$ to $V_s/V_{pi} = 2$. The effect of higher voltages with damping seems to decrease the difference for both switch designs by 19.3 μs and 27.48 μs depicting that the switching time converges at higher voltages.

REFERENCES

[1]. M. Bao, H. Yang, "Squeeze film air damping in MEMS", *Sens. Actuators A Phys*., vol. 136, pp. 3-27, May 2007.

[2]. M. I. Younis, MEMS Linear and nonlinear statics and dynamics, New York:Springer-Verlag, 2011.

[3]. T. Singh, "Design and finite element modeling of series-shunt configuration based RF MEMS switch for high isolation operation in K-Ka band", *Journal of Computational Electronics*, vol. 14, no. 1, pp. 167-179, March 2015.
[4]. N. Alcheikh, *et al.* "Influence of squeeze film damping on the higher-order modes of clamped–clamped microbeams." *Journal of Micromechanics and Microengineering* 26.6, pp. 065014, 2016.
[5]. C. Sri Harsha, C. S. R. Prasanth, and Pratiher B. "Effect of Squeeze Film Damping and AC Actuation Voltage on Pull-in Phenomenon of Electrostatically Actuated Microswitch." *Procedia Engineering*., vol.144, pp. 891-899, 2016.
[6]. Ouakad, Hassen M., Hussain M. Al-Qahtani, and Muhammad A. Hawwa. "Influence of squeeze-film damping on the dynamic behavior of a curved micro-beam." *Advances in Mechanical Engineering* 8, no. 6, pp. 1687814016650120, 2016.
[7]. Liu, Chin-Chia, and Cha'o-Kuang Chen. "Modeling and simulation of nonlinear micro-electromechanical circular plate." *Smart Science* 1, no. 1, pp. 59-63, 2013.
[8]. L. Mol, L. A. Rocha, E. Cretu, R. F. Wolffenbuttel, "Squeezed film damping measurements on a parallel-plate MEMS in the free molecule regime", *Proc. TRANSDUCERS*, pp. 1425-1428, 2009-Jun.-21–25.
[9]. E. Hosseinian, P. O. Theillet, and O. N. Pierron, "Temperature and humidity effects on the quality factor of a silicon lateral rotary micro-resonator in atmospheric air", *Sens. Actuators A*, vol. 189, pp. 380-389, Jan. 2013.
[10]. Paola Farnielli, Francesco Solazzi, Carlos Calaza, Benno Margesin, and Roberto Sorrentino, "A Wide Tuning Range MEMs Varactor Based on a Toggle Push-Pull Mechanism" in EuMIC, Amsterdam:, pp. 474-477, Oct. 2008.
[11]. Rebeiz, Gabriel M., and Jeremy B. Muldavin. "RF MEMS switches and switch circuits." *IEEE Microwave magazine* 2, no. 4:,pp. 59-71, 2001.
[12]. M. Bao, "Modified Reynolds equation and analytical analysis of squeeze-film air damping of perforated structures", *J. Micromech. Microeng*., vol. 13, no. 6, 2003.
[13]. Kumar A., P. Rudra, P. Fook, S. Chau, "Analytical solution of the modified Reynolds equation for squeeze film damping in perforated MEMS structures", *Sens. Actuators A Phys*., vol. 135, no. 2, pp. 839-848, 2007.
[14]. T. Veijola, H. Kuisma, J. Lahdenpera, T. Ryhanen, "Equivalent-circuit model of the squeezed gas film in a silicon accelerometer", *Sens. Actuators A Phys.*, vol. 48, pp. 239-248, May 1995.
[15]. P.T Tsilingiris, Thermophysical and transport properties of humid air at temperature range between 0 and 100 C. "*Energy Conversion and Management*, 49(5), pp.1098-1110, 2008.